ACS Catalysis

RESEARCH ARTICLE

pubs.acs.org/acscatalysis

Replacing Platinum with Tungsten Carbide (WC) for Reforming Reactions: Similarities in Ethanol Decomposition on Ni/Pt and Ni/WC Surfaces

Hui Ren,[†] Danielle A. Hansgen,[‡] Alan L. Stottlemyer,[‡] Thomas G. Kelly,[‡] and Jingguang G. Chen*[,‡]

[†]Department of Chemistry and [‡]Department of Chemical Engineering, Center for Catalytic Science and Technology (CCST), University of Delaware, Newark, Delaware 19716, United States

ABSTRACT: Selective reforming of biomass-derived oxygenates to produce hydrogen or syngas (H_2 + CO) offers an attractive route for biomass utilization. As reported previously, the Ni/Pt(111) bimetallic surface, with one monolayer of Ni residing on top of Pt(111), showed enhanced activity in oxygenate reforming. However, the Ni/Pt(111) structure is not stable at high temperatures because of diffusion of Ni into bulk Pt. In the current study we explore the possibility of replacing the Pt substrate with tungsten monocarbide (WC) to prevent the diffusion of monolayer Ni into the bulk. We report a combined study using density functional theory (DFT), temperature programmed desorption (TPD), and high resolution electron energy loss spectroscopy (HREELS) to compare the reforming reaction of ethanol on Ni/Pt and Ni/WC surfaces. Strong similarities are observed in the reaction pathways of ethanol on monolayer Ni/Pt and Ni/WC, demonstrating the feasibility to replace Pt with WC and to use monolayer Ni/WC as active and less expensive reforming catalysts.

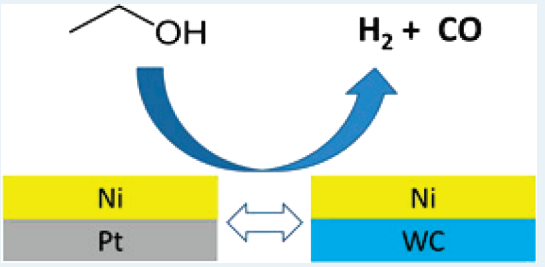

KEYWORDS: ethanol, reforming reaction, Ni/Pt, Ni/WC, bimetallic surfaces

1. INTRODUCTION

The production of hydrogen or syngas (H_2 + CO) from the selective reforming of biomass-derived oxygenates has been the subject of many recent studies.[1,2] The reforming process is potentially CO_2 neutral, as the CO_2 byproduct can be consumed by future biomass growth. Other advantages of oxygenate reforming include low toxicity and low reactivity of the oxygenates, which are compatible with the current infrastructure for transportation and storage. In our previous work, the reforming of ethanol, ethylene glycol, and glycerol was studied on Ni/Pt(111) single crystal surfaces to determine the effect of bimetallic formation on reforming activity.[3−6] The surface with a monolayer of Ni atoms residing on Pt(111) displayed higher reforming activity than either of the parent metal surfaces. The enhanced reforming activity was correlated to the electronic interaction and strain effects between the surface Ni monolayer and the Pt(111) substrate.[7] Along with surface science studies, investigations using supported catalysts showed that the Ni/Pt bimetallic catalyst supported on γ-Al_2O_3 displayed increased turnover frequencies for aqueous phase reforming of ethylene glycol compared to Pt/γ-Al_2O_3 at similar conditions.[8]

The surface science studies on Ni/Pt(111) bimetallic surfaces also revealed that the enhanced reforming activity disappeared after the surface monolayer Ni diffused into the Pt(111) substrate at 600 K.[5,6] It is therefore desirable to support the Ni monolayer on a substrate that is similar to Pt but with higher resistance to the diffusion of surface Ni atoms. Tungsten monocarbide (WC) has shown Pt-like properties in heterogeneous[9,10] and electrochemical reactions.[11] Furthermore, WC has been demonstrated as an effective diffusion barrier layer to prevent the inward diffusion of metal overlayers.[12] In a recent study it was reported that the surface Ni monolayer did not undergo thermally induced diffusion at temperatures up to 800 K.[15] These combined properties suggest that monolayer Ni on WC can potentially be a more thermally stable and less expensive alternative to Ni/Pt for the reforming of oxygenates.

In this work we use the reforming of ethanol as a probe reaction to compare the general similarities between monolayer Ni/WC and Ni/Pt surfaces to examine the feasibility of replacing the Pt substrate with WC. This is accomplished by carburizing a polycrystalline W foil followed by subsequent deposition of a Ni monolayer. To bridge the "materials gap" between the current polycrystalline Ni/WC surfaces with previous studies on single crystal Ni/Pt(111), ethanol reforming is also investigated on monolayer Ni on a polycrystalline Pt foil. Temperature programmed desorption (TPD) experiments are performed to provide a quantitative comparison of the reforming yield on Ni/Pt(111), polycrystalline Ni/Pt and Ni/WC surfaces. High-resolution electron energy loss spectroscopy (HREELS) is utilized to compare the reaction intermediates on the Ni/Pt and Ni/WC surfaces. Density functional theory (DFT) calculations are also performed to reveal similar binding energies of ethanol and the ethoxy (C_2H_5O) intermediate on Ni/Pt and Ni/WC surfaces.

2. EXPERIMENTAL AND DFT METHODS

2.1. Techniques. TPD and HREELS experiments were performed in two separate UHV chambers. The TPD chamber was

Received: February 3, 2011
Revised: February 24, 2011
Published: February 28, 2011

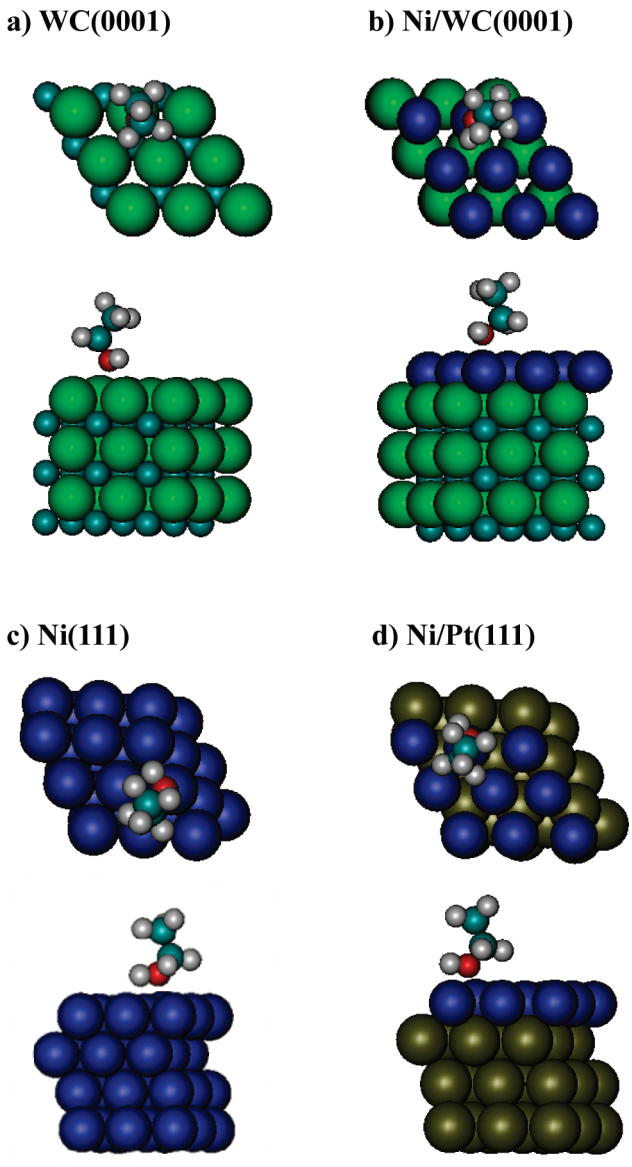

Figure 1. Ethanol binding configurations on (a) WC(0001), (b) Ni-WC(0001), (c) Ni(111), and (d) Ni−Pt−Pt(111) surfaces. White = hydrogen, red = oxygen, cyan = carbon, blue = nickel, green = tungsten, and brown = platinum.

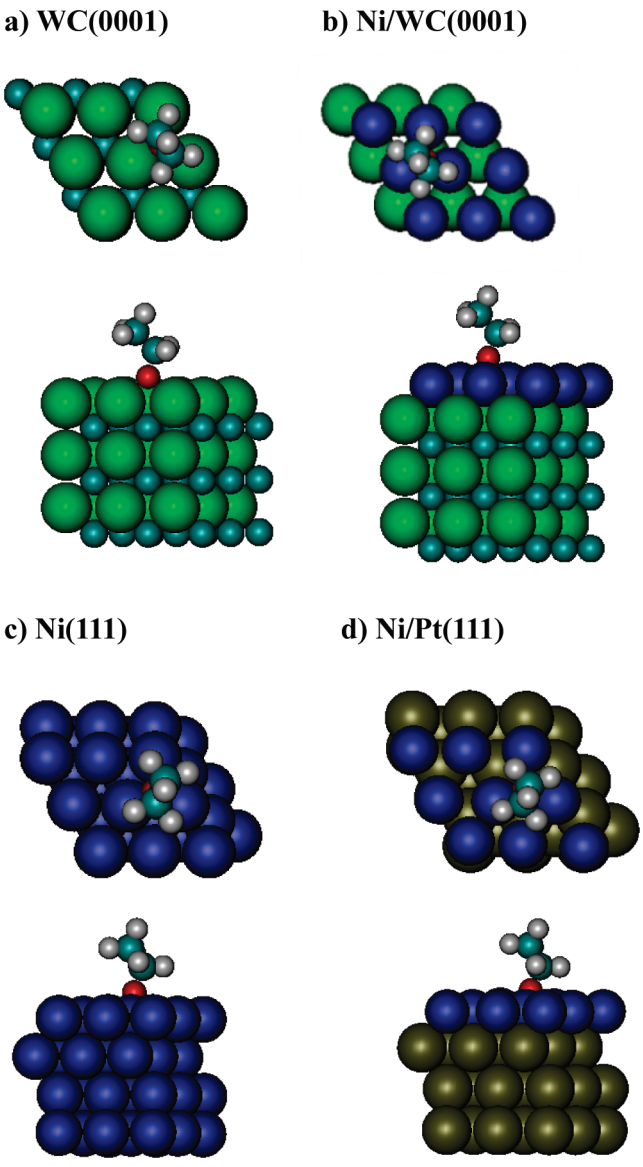

Figure 2. Ethoxy binding configurations on (a) WC(0001), (b) Ni-WC(0001), (c) Ni(111), and (d) Ni−Pt−Pt(111) surfaces. White = hydrogen, red = oxygen, cyan = carbon, blue = nickel, green = tungsten, and brown = platinum.

a two-level stainless steel chamber with a base pressure of 1×10^{-10} Torr. The chamber was equipped with a single-pass cylindrical mirror analyzer for Auger electron spectroscopy (AES) analysis, a sputter gun for cleaning, and a quadrapole mass spectrometer (QMS) for TPD experiments, as described previously.[13] The HREELS chamber was a three-level stainless chamber with a base pressure of 5×10^{-10} Torr. This chamber was equipped with an AES, sputter gun and QMS in the top two levels and HREELS in the bottom level, as described previously.[14]

The substrates studied were polycrystalline Pt foil (Alfa Aesar, 99.997%) and polycrystalline W foil (Alfa Aesar, 99.95%). Each foil was spot-welded to two tantalum posts which served as thermal and electrical conductors. By using resistive heating and liquid nitrogen cooling, the temperature could be controlled between 100 and 1200 K. A K-type thermocouple was spot-welded to the back of the foil to measure the sample temperature.

2.2. Preparation of Bimetallic Surfaces. To prepare a clean Pt or W surface, the sample was subjected to cycles of Ne^+ sputtering at 600 K and for Pt, followed by exposing to O_2 at 1050 K to remove residual carbon. This process was repeated until impurities were below the detection limits in the AES measurements. The clean WC surface was prepared by carburizing the W foil with cycles of ethylene sputtering at 300 K followed by annealing to 1200 K, as described previously.[15] The carburization process was repeated until a W:C stoichiometry of 1:1 as verified by AES.

Monolayer Ni was deposited on polycrystalline Pt and WC by thermally vaporizing Ni from a Ni source, which consisted of a 0.5 mm diameter tungsten wire (Alfa Aesar, 99.95%) wrapped with 0.1 mm diameter wire of Ni (Alfa Aesar, 99.95%). The Pt and WC surface temperature was held at 300 K during Ni deposition. The coverage of Ni was determined by using the

dx.doi.org/10.1021/cs200057y |ACS Catal. 2011, 1, 390–398

Table 1. Binding Energies of Ethanol, Ethoxy and Hydrogen (in kcal/mol) Along with the Position of the Most Stable Binding Site for the WC(0001), Ni/WC(0001), Ni/Pt(111), and Ni(111) Surfaces[a]

			bond length (Angstrom)				
adsorbate	surface	binding site	M−O	C−O	C−C	C−C−O bond angle (deg)	binding energy (kcal/mol)
ethanol	WC(0001)	atop	2.29	1.46	1.51	111.4	17.0
	Ni/WC(0001)	atop	2.13	1.46	1.51	111.6	13.5
	Ni/Pt(111)	atop	2.02	1.46	1.51	110.7	15.6
	Ni(111)	atop	2.20	1.46	1.51	111.6	6.9
ethoxy	WC(0001)	hcp	2.19	1.51	1.51	116.5	91.6
	Ni/WC(0001)	hcp	2.13	1.45	1.51	114.0	70.1
	Ni/Pt(111)	fcc	2.09	1.47	1.51	114.1	68.3
	Ni(111)	fcc	2.01	1.46	1.51	113.0	56.4
hydrogen	WC(0001)	fcc					77.6
	Ni/WC(0001)	hcp					68.1
	Ni/Pt(111)	fcc					69.0
	Ni(111)	fcc					64.7

[a] Additionally listed for ethanol and ethoxy are the bond lengths of the metal−oxygen, carbon−oxygen, and carbon−carbon bonds, and the carbon−carbon−oxygen bond angles.

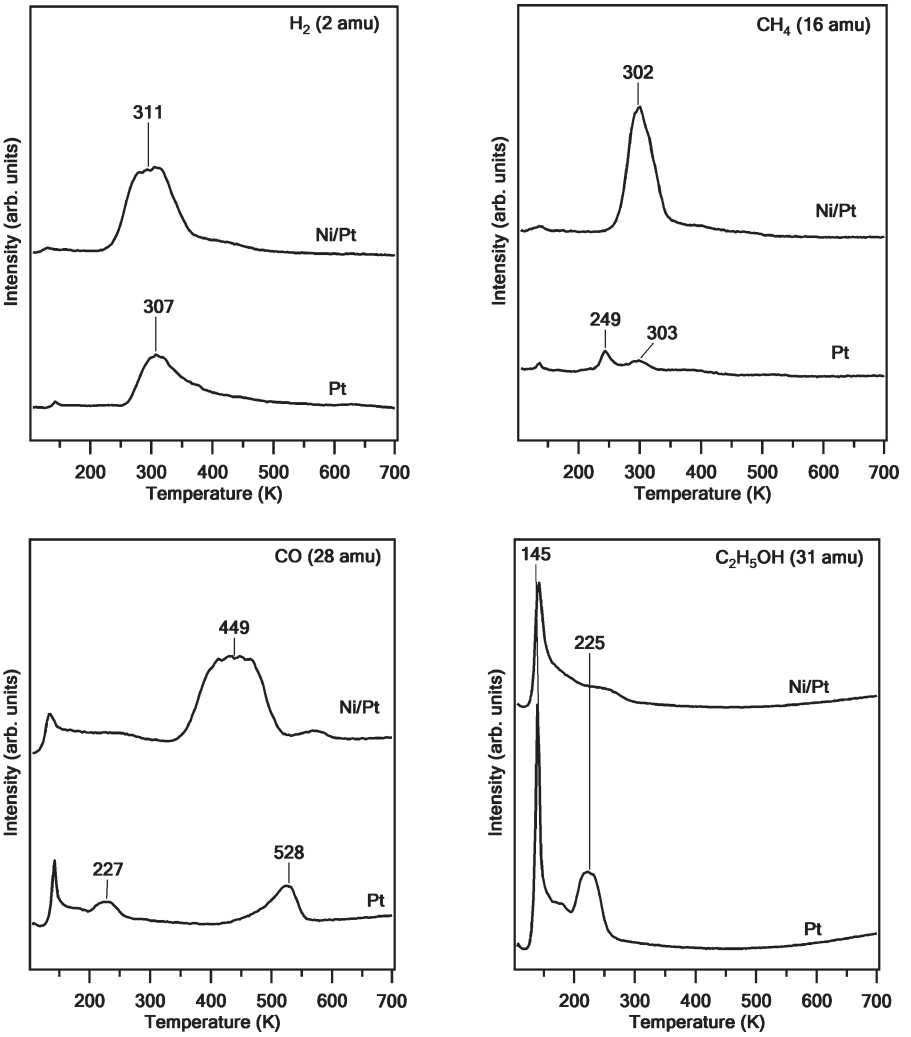

Figure 3. TPD spectra after 2 L exposure of C_2H_5OH on polycrystalline Pt and monolayer Ni/Pt surfaces.

dx.doi.org/10.1021/cs200057y |ACS Catal. 2011, 1, 390–398

Table 2. Quantification of TPD Results of C_2H_5OH Reactions on Different Surfaces

	Activity (ML)					
surface	reforming	decomposition	CH_4	ethylene	formaldehyde	total
Pt(111)	0.03	0	<0.01	0	0	0.03
1 ML Ni/Pt(111)	0.07	<0.01	0.01	0	0	0.09
Pt foil	0.01	0.03	<0.01	0	0	0.04
1 ML Ni/Pt foil	0.09	<0.01	0.04	0	0	0.13
WC foil	0	0.03	0	0.06	<0.01	0.09
1 ML Ni/WC	0.10	0.03	0.02	0	0	0.15
Thick Ni/WC	0.03	0.01	0.02	0	0	0.06

	Selectivity (%)				
surface	reforming	decomposition	CH_4	ethylene	acetaldehyde
Pt(111)	93	0	7	0	0
1 ML Ni/Pt(111)	85	3	12	0	0
Pt foil	32	68	0	0	0
1 ML Ni/Pt foil	68	5	27	0	0
WC foil	0	32	0	67	0.63
1 ML Ni/WC	65	23	12	0	0
Thick Ni/WC	49	21	30	0	0

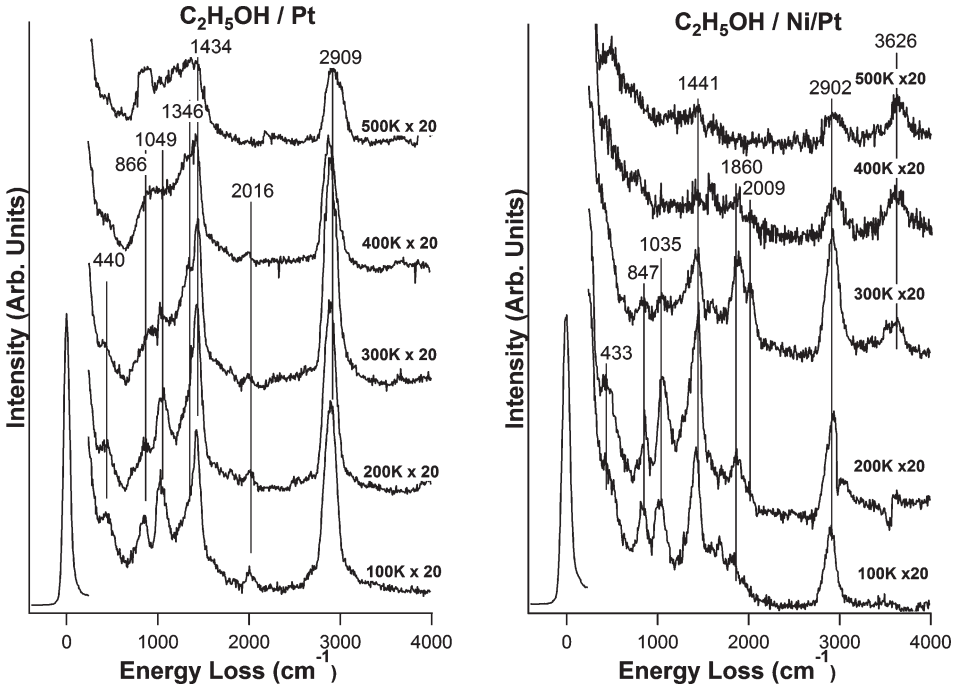

Figure 4. HREELS spectra monitoring the thermal decomposition of C_2H_5OH on polycrystalline Pt and monolayer Ni/Pt surfaces. The 3626 cm^{-1} feature on Ni/Pt at higher temperatures is due to the adsorption and decomposition of H_2O from the UHV background.

standard overlayer/substrate equations,[16] as described previously for the deposition of Ni on polycrystalline Pt[17] and WC.[15]

Monolayer coverage of C_2H_5OH (Sigma-Aldrich, 99.9+%) was achieved after 2 L (1 Langmuir (L) =1 × 10^{-6} Torr·s) exposure in the TPD chamber and 4 L in the HREELS chamber. The ethanol sample was purified by freeze−pump−thaw cycles before use. C_2H_5OH was dosed at a substrate temperature of 100 K. The TPD experiments were then performed by ramping the temperature from 100 to 800 K with a linear heating rate of 3 K/s, with up to 12 masses being simultaneously monitored. The HREELS measurements were performed after flashing the surface to the temperature of interest at 3 K/s, and the spectra were recorded after the surface was cooled back to 100 K.

2.3. DFT Calculations. DFT calculations were performed using the Vienna ab initio Simulation Package (VASP) version 4.6.[18,19] The PW-91 functional[20] was used with ultrasoft Vanderbilt pseudopotentials[21] and an energy cut off of 396 eV. All

dx.doi.org/10.1021/cs200057y |ACS Catal. 2011, 1, 390–398

Table 3. Vibrational Assignments for Ethanol on Pt, Ni/Pt, WC, and Ni/WC Surfaces

mode	gas phase[29]	solid phase[30]	Pt(111)[6]	Pt Foil	Ni/Pt Foil	WC	Ni/WC
δ(CCO)		419	450	440	433		
γ(OH)							
$\gamma(CH_2)$		801	800				
ν_s(CCO)	880	885	880	866	847	879	873
$\rho(CH_3)$		1033					
ν_{as}(CCO)	1060	1089	1060	1049	1035	1062	1055
δ(OH)		1241					
$\delta_s(CH_3)$	1390	1394		1346		1366	1373
$\delta_{as}(CH_3)$		1452					
$\delta(CH_2)$	1450	1490	1450	1434	1441	1448	1434
ν(CO), M-CO			2080	2016	1860, 2009		
$\nu(CH_2)$		2900					
$\nu_s(CH_3)$	2880	2943					
$\nu_{as}(CH_3)$	2965	2989	2960	2909	2902	2902	2916
ν(OH)	3660	3676	3230		3626		

slab calculations were performed using a 3 × 3 unit cell with a 5 × 5 × 1 Monkhorst−Pack k-point grid. Bulk lattice constants were optimized for the hexagonal closed packed (hcp) form of WC and were found to be $a = b = 2.92$ Å and $c = 2.84$ Å which are in agreement with experimental lattice constants ($a = b = 2.91$ Å, $c = 2.84$ Å).[22] Binding energies were calculated on the tungsten-terminated WC(0001) surface with three layers each of alternating tungsten and carbon. The topmost tungsten layer and carbon layer were relaxed, while the remaining layers were frozen. For the Ni/WC(0001) system, a pseudomorphic layer of Ni atoms was added to the top of the WC(0001) surface and was found to be most stable in the hcp sites. For the Pt and Ni/Pt bimetallic surfaces, the previously optimized lattice constant value of 4.01 Å was used. The Ni/Pt system was composed of a Pt(111) bulk of three layers with one Ni layer on top. For these calculations, the top two metal layers were allowed to relax, and the bottom two were kept frozen. The binding energies were calculated through the following equation:

$$\Delta E_{adsorbate} = E_{(slab\ +\ adsorbate)} - E_{(slab)} - E_{(adsorbate)}$$

Where $E_{(slab)}$ is the energy of the clean slab, $E_{(adsorbate)}$ is the energy of the adsorbate in vacuum, and $E_{(slab+adsorbate)}$ is the energy of the slab with the adsorbate. All binding energies were extrapolated to $k_BT = 0$ eV.

3. RESULTS AND DISCUSSION

3.1. DFT Calculations of Binding Energies. Ethanol decomposition has been studied experimentally on Pt(111)[3,4,23−26] and Ni(111)[27,28] under UHV conditions. On both surfaces the initial step for ethanol dissociation is O−H bond scission to produce adsorbed ethoxy and atomic hydrogen. For this reason the binding energies of ethanol, ethoxy, and hydrogen are calculated in the current study to compare the similarities and differences between monolayer Ni/Pt and Ni/WC. The atop, bridge, fcc, and hcp binding sites were all considered for ethanol, ethoxy, and atomic hydrogen on each surface to identify the most stable binding configuration (lowest Gibbs free energy). Figures 1 and 2 show the preferred binding configurations of ethanol and ethoxy, respectively, on each of the surfaces. Ethanol prefers to bind in the atop site, whereas ethoxy prefers to bind in a 3-fold site, either the fcc or the hcp site depending on the surface.

The distance between the Ni layer and WC bulk was found to be 1.87 Å. This is slightly lower than the Ni−Pt distance of 1.99 Å. Upon adding ethanol or ethoxy, the Ni atoms that the molecule is bound to moved up out of the surface slightly, increasing the Ni −WC layer distance to 1.96 Å and 1.92 Å, respectively. The behavior of the Ni/Pt surface was similar, with the Ni−Pt distance increasing to 2.10 Å and 2.04 Å, respectively. For all Ni atoms unbound to either ethanol or ethoxy, the Ni−WC and Ni−Pt distance remained unchanged.

The binding energies of ethanol, ethoxy, and hydrogen on different surfaces are compared in Table 1 along with the adsorbate geometries. For the 3-fold coordinated ethoxy species, the metal−oxygen bond length was averaged over the three metal−oxygen bonds. Comparing the binding energies, the unmodified WC surface bonds to all three adsorbates more strongly than the other surfaces. In comparison, the Ni(111) surface shows the weakest binding energies. Most interestingly, the binding energies on Ni/WC are very similar to Ni/Pt for all three adsorbates. This observation suggests that the monolayer Ni/WC and Ni/Pt surfaces would most likely have similar activities toward the surface reaction of ethanol, as confirmed experimentally below.

3.2. Ethanol Reaction on Ni/Pt Surfaces. The TPD spectra following the decomposition of C_2H_5OH on polycrystalline Pt and Ni/Pt surfaces are shown in Figure 3. The desorption of C_2H_5OH occurs at approximately 145 and 225 K for physisorbed multilayer and chemisorbed monolayer, respectively. Comparing with Pt, the desorption peak at 225 K is very weak on Ni/Pt, suggesting that chemisorbed C_2H_5OH undergoes reaction instead of desorption. The decomposition of C_2H_5OH leads to the desorption of H_2 at 307 and 311 K from Pt and Ni/Pt, respectively. On Pt, CO desorbs at 227 and 528 K, and trace amounts of CH_4 are observed at 249 and 303 K. On Ni/Pt, CO desorbs at 449 K and CH_4 desorbs at 302 K. The peak areas of all three products are larger from Ni/Pt than Pt. In particular, the detection of relative intense desorption peaks of CO and CH_4

dx.doi.org/10.1021/cs200057y |ACS Catal. 2011, 1, 390–398

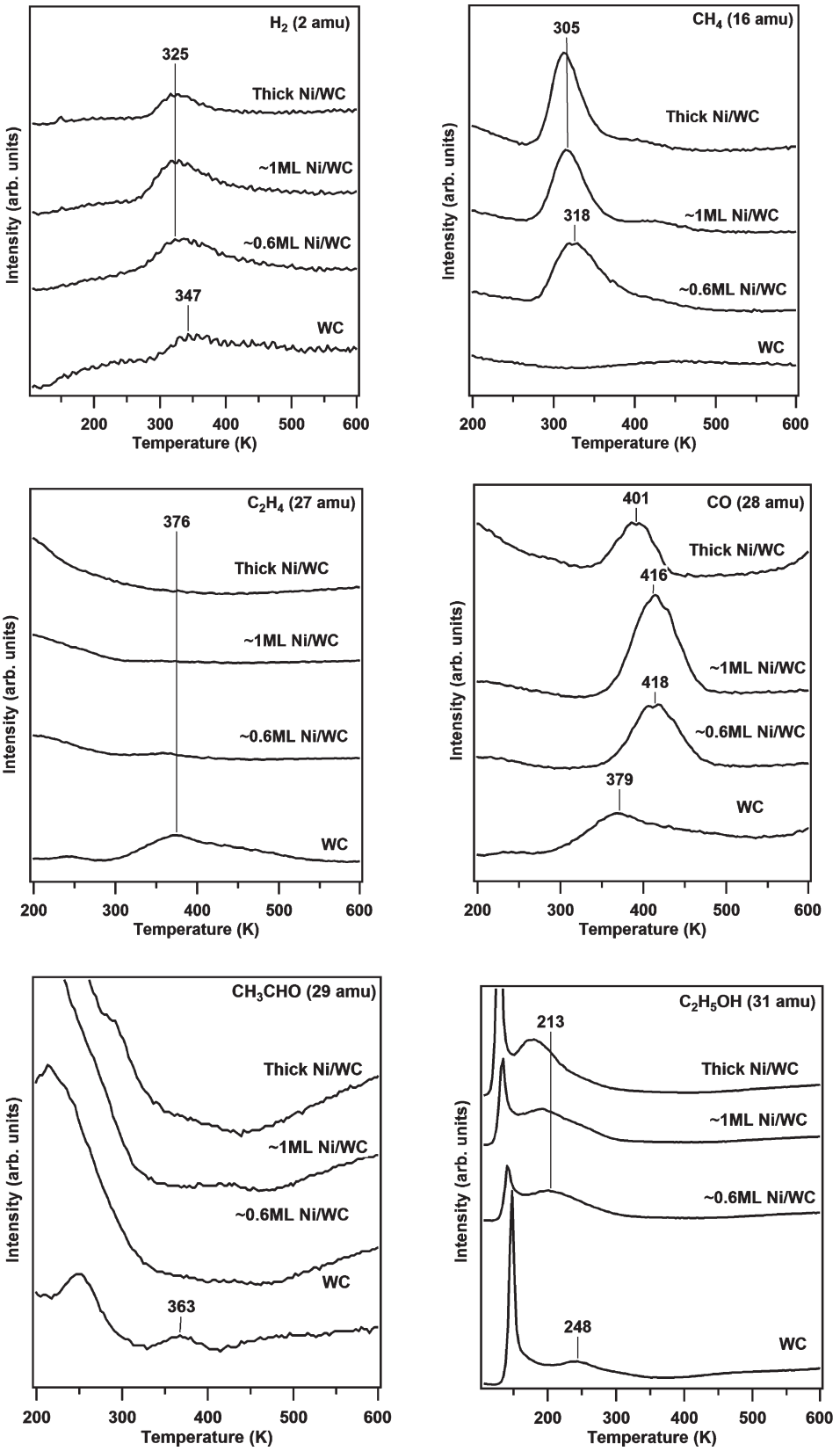

Figure 5. TPD results after 2 L C_2H_5OH exposure on WC and Ni modified WC surfaces.

indicates that the monolayer Ni/Pt surface is active to C−C bond scission. This is consistent with previous single crystal studies where the monolayer Ni/Pt(111) surface was more active to C−C scission than pure Pt(111).[5]

dx.doi.org/10.1021/cs200057y |*ACS Catal.* 2011, 1, 390–398

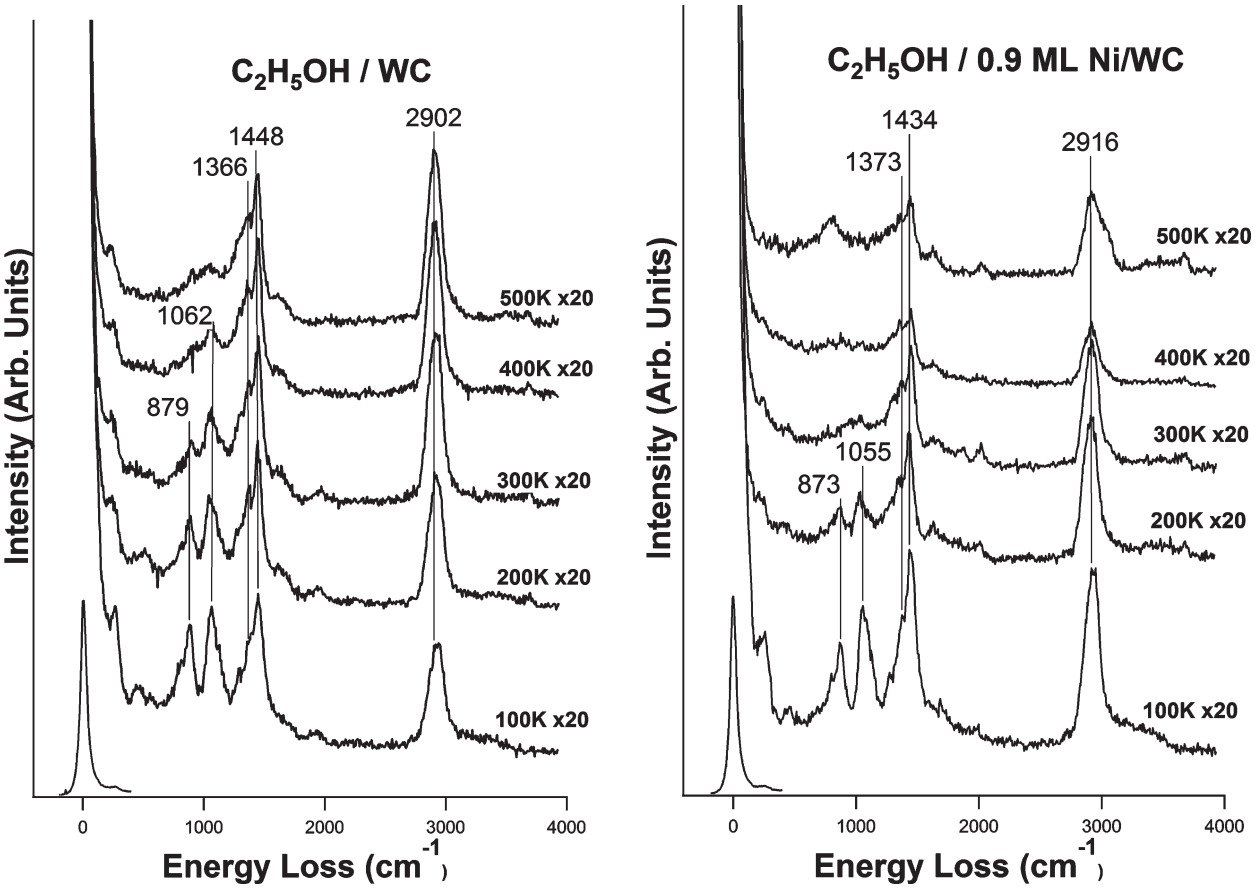

Figure 6. HREELS spectra monitoring the thermal decomposition of C_2H_5OH on WC and Ni/WC surfaces.

The TPD results in Figure 3 suggest that C_2H_5OH decomposes on Pt and Ni/Pt via the following three reaction pathways:

$$\text{Reforming} \qquad C_2H_5OH \rightarrow CO + 3H_2 + C_{ads} \qquad (1)$$

$$\text{Total Decomposition} \qquad C_2H_5OH \rightarrow 2C_{ads} + O_{ads} + 3H_2 \qquad (2)$$

$$\text{Methane Production} \qquad C_2H_5OH \rightarrow CO + H_2 + CH_4 \qquad (3)$$

Using similar procedures described previously on Ni/Pt(111) surfaces,[5] the activity and selectivity of C_2H_5OH decomposition are quantified from the TPD peak areas. These results are compared in Table 2 with the corresponding single crystal surfaces. Comparing to Pt(111), the Pt foil shows a lower yield in CO production and higher activity toward total decomposition, most likely because of the presence of defects and undercoordinated sites on the Pt foil that are active to C−O bond scission. As compared in Table 2, the TPD results reveal general similarities between monolayer Ni/Pt(111) and Ni/Pt polycrystalline surfaces, with both showing a high activity toward reforming and negligible activity for total decomposition. The main difference between the two surfaces is the higher CH_4 yield on the polycrystalline Ni/Pt surface.

HREELS measurements were performed to identify the surface reaction intermediates and to gain better understanding of the reaction pathways; the spectra are shown in Figure 4. The assignments of vibrational peaks of C_2H_5OH on these surfaces are summarized in Table 3. At 100 K, the vibrational features on both Pt and monolayer Ni/Pt polycrystalline surfaces are similar to those expected for C_2H_5OH, with the exception that the ν(O−H) mode is absent, suggesting that the O−H bond scission has occurred to produce the surface ethoxy intermediate. This observation is consistent with previous HREELS detection of ethoxy on the corresponding single crystal surfaces.[6] Upon heating to higher temperatures, features associated with the CCO group, namely, the ν_s(CCO) and ν_{as}(CCO) modes, decrease in intensity and peaks are detected at 2016 cm^{-1} on Pt and at 1860 and 2009 cm^{-1} on Ni/Pt. These peaks are assigned to the ν(CO) mode of the CO product from the dissociation of ethoxy. The relative intensity of the ν(CO) mode is higher on Ni/Pt than on Pt, consistent with the TPD results of higher reforming activity on the Ni/Pt bimetallic surface. The feature at 3626 cm^{-1} on the Ni/Pt surface at higher temperatures is resulting from the dissociative adsorption of H_2O from the UHV background during data acquisition.

3.3. Ethanol Reaction on Ni-WC Surfaces. The TPD results following the decomposition of ethanol on WC and Ni/WC are shown in Figure 5. Four surfaces were studied, pure WC, 0.6 ML Ni/WC, 1 ML Ni/WC, and a thick Ni film (>5 ML) prepared on WC to provide a reference of chemistry on Ni surfaces. Monolayer C_2H_5OH desorbed from both Ni/WC surfaces at 213 K, which was slightly lower compared to the desorption temperature of 248 K from the WC surface. A higher desorption

dx.doi.org/10.1021/cs200057y |ACS Catal. 2011, 1, 390–398

temperature of C_2H_5OH on WC implied a stronger binding between C_2H_5OH molecules and WC substrate, consistent with DFT calculations. The H_2 product desorbed at 347 K from WC and at 325 K from the Ni/WC surfaces. CH_4 generation was observed from Ni/WC surfaces but not from from WC, indicating that Ni/WC surfaces are active to C−C bond scission and CH_4 production, similar to the Ni/Pt surface. Considering that both C_2H_4 and CO molecules could contribute to the cracking patterns of 28 amu, 27 amu was used to measure C_2H_4 production. By normalizing the intensity of 27 to 28 amu peak based on calibration of gas-phase C_2H_4 in the same UHV system, the amount of CO and C_2H_4 production can be quantified separately. It was determined that the 28 amu peak observed on WC surface was all from C_2H_4 production, indicating the absence of reforming reaction pathway on WC. Moreover, different from Ni/WC, the WC surface generated C_2H_4 (27 amu) as the main reaction product. Another reaction pathway on WC was the production of trace amount of acetaldehyde (CH_3CHO, 29 amu). The quantification of the gas-phase yields of the various products is summarized in Table 2.

Overall, results in Table 2 reveal that the main reaction pathways on the WC surface are total decomposition and ethylene production, with a selectivity of 32% and 67%, respectively. Upon the modification with Ni, the reforming activity increases, and ethylene production disappears on the one ML Ni/WC surface. The TPD results in Figure 5 also reveal that the characteristic reaction pathways on WC, such as the production of C_2H_4 and the inhibition to CH_4 production, disappear at a Ni coverage of 0.6 ML. This observation suggests that even submonolayer coverage of Ni can significantly alter the chemical properties of WC. Furthermore, the monolayer Ni/WC surface shows higher reforming activity than both WC and the thick Ni film, indicating a synergistic effect from the interaction of monolayer Ni with the WC substrate.

Figure 6 shows the HREELS spectra of C_2H_5OH on WC and 0.9 ML Ni/WC surfaces. Using similar peak assignments described in Table 3, ethanol adsorbs dissociatively on both surfaces, as indicated by the absence of the ν(OH) mode. The peaks due to ν_s(CCO) at 879 cm^{-1} and ν_{as}(CCO) at 1062 cm^{-1} were present on the WC surface until 400 K. In comparison, on the Ni/WC surface those peaks disappeared by 300 K, leaving only modes due to CH_x. The presence of Ni on WC substantially increases the activity toward breaking the C−C bond, consistent with the trend observed from TPD measurements.

3.4. Comparison of Monolayer Ni/Pt and Ni/WC Surfaces. The monolayer Ni/Pt and Ni/WC surfaces show several similarities in the reactions of ethanol: (1) DFT calculations (Table 1) indicate similar binding energies of ethanol, ethoxy, and atomic hydrogen between the two surfaces, suggesting a similar initial decomposition pathway of ethanol. (2) HREELS results (Figures 4 and 6) confirm that the O−H bond scission occurs on both surfaces, leading to the formation of the ethoxy intermediate that subsequently decomposes to produce CO and H_2. (3) Quantification from the TPD peak areas (Table 2) provides similar reaction pathways, with reforming reaction being the dominant pathway on these surfaces and with an activity of 0.09 ML on Ni/Pt and 0.10 ML on Ni/WC.

The two surfaces also show some differences. For example, DFT results reveal minor differences in the preferred bonding sites of ethoxy, with the fcc sites on Ni/Pt(111) and hcp sites on Ni/WC(0001). Another difference is that the CO product is detected as a surface intermediate on Ni/Pt (Figure 4) but not on Ni/WC (Figure 6). However, these differences do not appear to significantly affect the decomposition pathways of ethoxy, as revealed by the TPD results (Figures 3 and 5) showing similar desorption temperature ranges of H_2 (311 K on Ni/Pt and 325 K on Ni/WC), CO (~449 K on Ni/Pt and 416 K on Ni/WC), and CH_4 (302 K on Ni/Pt and 305 K on Ni/WC).

The most important observation from the current study is that both monolayer Ni/Pt and Ni/WC show higher reforming activity than the monometallic Pt and Ni surfaces (Table 2). This confirms that the reforming pathway on Pt can be enhanced by the formation of Ni/Pt bimetallic surfaces, and more importantly, that the Pt substrate can be replaced by WC. The monolayer Ni/WC system represents a promising catalyst that is Pt-free and is potentially selective for the reforming of oxygenates. Synthesis and reactor evaluation of supported Ni/WC catalysts are needed to verify such prediction.

4. CONCLUSIONS

A combination of DFT calculations and surface science experiments was used to determine the feasibility of replacing the bulk Pt of the Ni/Pt bimetallic surface with WC for the reforming of oxygenates. The following conclusions can be made based on the results and discussion presented above:

(1) The Ni/Pt polycrystalline surface shows similar reaction pathways to those observed on single crystal Ni/Pt(111), demonstrating general similarities between model and more complex surfaces for the reforming reaction of ethanol.
(2) The dominant reaction pathway of ethanol on unmodified WC surface is the production of ethylene, suggesting that most of surface sites are relatively inert to C−C bond cleavage but active for C−O and C−H bond scission. The selectivity toward C−O bond scission should make WC a promising catalyst for the deoxygenation of oxygenates such as alcohols and polyols.
(3) General similarities are observed in the reaction pathways of ethanol on monolayer Ni/Pt and Ni/WC, demonstrating the feasibility to replace Pt with WC and to use monolayer Ni/WC as active and less expensive reforming catalysts.

AUTHOR INFORMATION

Corresponding Author
*E-mail: jgchen@udel.edu.

ACKNOWLEDGMENT

This work was supported by the Department of Energy, Office of Basic Energy Sciences (DOE/BES Grant DE-FG02-00ER15104).

REFERENCES

(1) Davda, R. R.; Shabaker, J. W.; Huber, G. W.; Cortright, R. D.; Dumesic, J. A. *Appl. Catal., B* **2005**, *56*, 171–186.
(2) Huber, G. W.; Iborra, S.; Corma, A. *Chem. Rev.* **2006**, *106*, 4044–4098.
(3) Skoplyak, O.; Barteau, M. A.; Chen, J. G. *ChemSusChem* **2008**, *1*, 524–526.
(4) Skoplyak, O.; Menning, C. A.; Barteau, M. A.; Chen, J. G. *Top. Catal.* **2008**, *51*, 49–59.

(5) Skoplyak, O.; Barteau, M. A.; Chen, J. G. *J. Phys. Chem. B* **2006**, *110*, 1686–1694.
(6) Skoplyak, O.; Barteau, M. A.; Chen, J. G. *Surf. Sci.* **2008**, *602*, 3578–3587.
(7) Chen, J. G.; Menning, C. A.; Zellner, M. B. *Surf. Sci. Rep.* **2008**, *63*, 201–254.
(8) Huber, G. W.; Shabaker, J. W.; Evans, S. T.; Dumesic, J. A. *Appl. Catal., B* **2006**, *62*, 226–235.
(9) Levy, R. B.; Boudart, M. *Science* **1973**, *181*, 547–549.
(10) Hwu, H. H.; Chen, J. G. *Chem. Rev.* **2005**, *105*, 185–212.
(11) Weigert, E. C.; Stottlemyer, A. L.; Zellner, M. B.; Chen, J. G. *J. Phys. Chem. C* **2007**, *111*, 14617–14620.
(12) Gouy-Pailler, P.; Pauleau, Y. *J. Vac. Sci. Technol., A* **1993**, *11*, 96–102.
(13) Liu, N.; Rykov, S. A.; Chen, J. G. *Surf. Sci.* **2001**, *487*, 107–117.
(14) Hwu, H. H.; Chen, J. G.; Kourtakis, K.; Lavin, J. G. *J. Phys. Chem. B* **2001**, *105*, 10037–10044.
(15) Humbert, M. P.; Menning, C. A.; Chen, J. G. *J. Catal.* **2010**, *271*, 132–139.
(16) Cumpson, P. J.; Seah, M. P. *Surf. Interface Anal.* **1997**, *25*, 430–446.
(17) Menning, C. A.; Chen, J. G. *J. Chem. Phys.* **2008**, *128* 164703–164709.
(18) Kresse, G.; Furthmüller, J. *Comput. Mater. Sci.* **1996**, *6*, 15–50.
(19) Kresse, G.; Furthmuller *Phys. Rev. B* **1996**, *54*, 11169–11186.
(20) Perdew, J. P.; Chevary, J. A.; Vosko, S. H.; Jackson, K. A.; Pederson, M. R.; Singh, D. J.; Fiolhais, C. *Phys. Rev. B* **1992**, *46*, 6671–6687.
(21) Vanderbilt, D. *Phys. Rev. B* **1990**, *41*, 7892–7895.
(22) Toth, L. E., *Transition Metal Carbides and Nitrides*; Academic Press: New York, 1971.
(23) Lee, A. F.; Gawthrope, D. E.; Hart, N. J.; Wilson, K. *Surf. Sci.* **2004**, *548*, 200–208.
(24) Panja, C.; Saliba, N.; Koel, B. E. *Surf. Sci.* **1998**, *395*, 248–259.
(25) Rendulic, K. D.; Sexton, B. A. *J. Catal.* **1982**, *78*, 126–135.
(26) Sexton, B. A.; Rendulic, K. D.; Hughes, A. E. *Surf. Sci.* **1982**, *121*, 181–198.
(27) Gates, S. M.; Russell, J. N., Jr.; Yates, J. T., Jr. *Surf. Sci.* **1986**, *171*, 111–134.
(28) Xu, J.; Zhang, X.; Zenobi, R.; Yoshinobu, J.; Xu, Z.; Yates, J. T., Jr. *Surf. Sci.* **1991**, *256*, 288–300.
(29) Sexton, B. A. *Surf. Sci.* **1979**, *88*, 299–318.
(30) Barnes, A. J.; Hallam, H. E. *Faraday Trans.* **1970**, *66* 1932–1940.